Original Article
Cancer stem cell vaccine expressing ESAT-6-gpi and IL-21 inhibits melanoma growth and metastases

Fengshu Zhao[1*], Xiangfeng He[2*], Jianan Sun[1*], Di Wu[1], Meng Pan[1], Miao Li[1], Songyan Wu[1], Rong Zhang[1], Chunguang Yan[1], Jun Dou[1]

[1]Department of Pathogenic Biology and Immunology, School of Medicine, Southeast University, Nanjing 210009, China; [2]Department of Medical Oncology, Affiliated Tumor Hospital of Nantong University, Nantong 226361, China. *Equal contributors

Abstract: Tumor vaccines may induce antitumor efficacy, however, weak immunogenicity of tumor antigens is one of the prime obstacles for excitation of the antitumor immune responses. Therefore, strategies that enhance immunogenicity of tumor vaccines are of particular interest. In this study, a novel melanoma B16F10 CD133$^+$CD44$^+$ cancer stem cell (CSC) vaccine expressing 6 kDa early secreted antigenic target (ESAT-6) in the glycosylphosphatidylinositol (GPI)-anchored form and secreting interleukin (IL)-21 was developed. Its anti-melanoma efficacy and mechanisms were investigated in mice. The results demonstrated that the B16F10-ESAT-6-gpi/IL-21 CD133$^+$CD44$^+$ CSC vaccine exhibited enhanced anti-melanoma efficacy as determined by inhibited melanoma growth, prolonged survival of melanoma bearing mice. The anti-melanoma immunity was associated with elevated levels of serum anti-ESAT-6 and interferon (IFN)-γ as well as increased cytotoxic activities of natural killer cells, splenocytes, and complement dependent cytotoxicity. Furthermore, this CSC-based vaccine apparently inhibited melanoma lung metastasis by decreasing the level of Vimentin while increasing the level of E-cadherin expression, suggesting an inhibited epithelial mesenchymal transition. Thus, the B16F10-ESAT-6-gpi/IL-21 CD133$^+$CD44$^+$ CSC vaccine may be used to reactivate the anti-tumor immunity and for treatment of melanoma.

Keywords: Melanoma, cancer stem cells, cancer stem cell vaccine, ESAT-6, interleukin-21

Introduction

Melanoma is an aggressive malignancy with a deplorable penchant for extensive metastasis. When melanoma spreads throughout human body, there is currently no reliable therapy for advanced metastatic melanoma. Novel strategies for the treatment of advanced malignant melanoma are clearly needed [1-3].

Although melanoma is a prototype of immunogenic tumor, melanoma- specific vaccines have demonstrated minimal clinical efficacy in patients with established disease. Thus, there is a need for research in the vaccine design, adjuvant selection as well as patient selection criteria [4-6]. Moreover, tumor vaccines against melanoma require immune tolerance break since tumor-associated antigens used in vaccine formula are mostly self-antigens [7-9]. To overcome the low immunogenicity limitation of

melanoma vaccine developed, a modified xenogeneic tumor vaccine and cytokine potent activator as well as sequencing for tailored melanoma vaccine might break immune tolerance and enhance the immunogenicity of melanoma vaccine for inducing melanoma-specific immune responses [9-11].

It is known that 6 kDa early secreted antigenic target (ESAT-6) is one of the most immunodominant mycobacterium tuberculosis-specific antigens that contain multiple immunogenic T/B cell epitopes. ESAT-6 has been shown to act as a xenogeneic antigen to break immune tolerance to melanoma in melanoma bearing body. [10, 12] Meanwhile, interleukin (IL)-21 is a pleiotropic cytokine that regulates the activity of both innate and adaptive immune responses. IL-21 stimulates T and natural killer (NK) cell proliferation and function and regulates B cell survival and differentiation and the function of

dendritic cells [13, 14]. Glycosylphosphatidylinositol (GPI) is a posttranslationally added lipid anchor and GPI-anchored membrane cytokines have been shown to play an important role in host immune response against tumor cells [15, 16]. In the previous study, we developed a melanoma B16F10 vaccine that expresses a ESAT-6 in the GPI-anchored form together with secreting IL-21 (B16F10-ESAT-6-gpi/IL-21 vaccine), which elicited an anti-ESAT-6 specific immune responses that decreased melanoma growth in the immunized C57BL/6 mice. However, this tumor vaccine failed to completely inhibit B16F10 melanoma growth and resulted in lung tumor metastases in mice [9].

There is increasing evidence that the cancer stem cells (CSCs) represent a minor population of self-renewing cancer cells that fuel tumor growth and a poor prognosis [17, 18]. CSCs are likely to be responsible for tumor-initiating potential, invasion, metastasis, resistance to traditional therapies and eventual relapse. CSC model can comprehensibly explain essential and insufficiently understood clinical events, such as therapy resistance, tumor recurrence and non-effective tumor vaccines [19, 20]. Recent studies suggest that CSC-based vaccines inhibit metastases of primary tumors by inducing humoral and cellular immune responses that result in lysis of these target CSCs [21-23]. Here, we describe the development and evaluation of the modified melanoma B16F10-ESAT-6-gpi/IL-21 CD133$^+$CD44$^+$ CSC vaccine, and aim to determine whether this ESAT-6-gpi and IL-21 expressed CSC vaccine was better than B16F10-ESAT-6-gpi/IL-21 vaccine in anti-melanoma efficacy. Our results demonstrate that compared with other vaccines, B16F10-ESAT-6-gpi/IL-21 CD133$^+$CD44$^+$ CSC vaccination significantly stimulated the anti-melanoma immunity which resulted in inhibited tumor growth and decreased lung metastasis in the melanoma bearing mice.

Materials and methods

Mice and cell lines

6-8 week of C57BL/6 mice were ordered from the Yangzhou University of China. All mice were housed under the pathogen-free condition and all experiments were performed in compliance with the guidelines of the Animal Research Ethics Board of Southeast University. B16F10 murine melanoma cell line is syngeneic in C57BL/6 mice and YAC-1 cell line is Moloney leukemia-induced T-cell lymphoma of A/Sn mouse origin. These cells were ordered from the Cellular Institute of China in Shanghai, and were cultured at 37°C in 5% CO_2 atmosphere in RPMI 1640 supplemented with 10% fetal bovine serum that contained 100 Uml^{-1} penicillin G sodium and 100 mg ml^{-1} streptomycin sulfate.

Clonal selection, identification and isolation of CD133$^+$CD44$^+$ cells

The constructed recombinant plasmid pIRES-ESAT-6-gpi/IL-21 was transfected into B16F10 cells by using Lipofectamine™ 2000 reagent (Invitrogen, USA) according to the manufacturer's protocol. The stably transfected clones were selected from RPMI containing 800 mg/ml G418 (Clontech, CA), and were cloned into cell line by limiting dilution. The clones expressing ESAT-6-gpi and IL-21 were identified by an immunofluorescence and immunoblotting techniques. B16F10-ESAT-6-gpi/IL-21 CD133$^+$CD44$^+$ double positive cells were isolated from B16F10-ESAT-6-gpi/IL-21 cells with magnetic activated cell sorting (MACS) method that was performed as described previously [24, 25]. Briefly, CD44$^+$CD133$^+$ double positive subsets were isolated from B16F10-ESAT-6-gpi/IL-21 cells using the primary monoclonal antibodies (rat anti-mouse CD44 or CD133-FITC, eBioscience Company, USA). Cells were washed twice in PBS, and were put the secondary monoclonal antibody (goat anti-rat coupled to magnetic microbeads, Miltenyi Biotec, Bergisch Gladbach, Germany). The isolated CD44$^+$CD133$^+$ double positive cells were named as B16F10-ESAT-6-gpi/IL-21 CD44$^+$CD133$^+$ CSCs [24].

Vaccine immunization and in vivo tumorigenicity experiments

The C57BL/6 mice were immunized with 5×10^5 B16F10-ESAT-6-gpi/IL-21 CD133$^+$CD44$^+$ CSC vaccine three times with interval of 14 days between the immunizations. All mice were challenged subcutaneous (s.c.) with 5×10^5 B16F10 cells 10 days after final immunization. As controls, B16F10 CD133$^+$CD44$^+$ CSCs, B16F10-ESAT-6-gpi/IL-21 CD133$^-$CD44$^-$ non CSCs, and B16F10-ESAT-6-gpi/IL-21 cell vaccines were used in vivo tumorigenicity experiments. All

vaccines were inactivated with mitomycin C (50 µg/ml) for 4 hours. Six mice/group were used in the experiments. Except for observation of mouse general conditions each day, tumor growth was monitored once every 5 days by measuring two perpendicular tumor diameters using calipers and then the tumor-free mice and survival mice were investigated, respectively [26].

Enzyme-linked immunosorbent assay (ELISA)

The levels of anti-ESAT-6 antibody and IFN-γ were detected by using ELISA Kit according to the manufacturer's protocol (BD eBioscience, San Jose, CA). The Kit is suitable for detecting samples that include cell culture supernatant and serum [27].

Complement dependent cytotoxicity (CDC) assay

For the determination of CDC activity, 2×10^5 B16F10 CD133+CD44+ CSCs, B16F10-ESAT-6-gpi/IL-21 CD133-CD44- non CSCs, B16F10/ESAT-6-GPI-IL-21 cells, and B16F10/ESAT-6-GPI-IL-21 CD133+CD44+ CSCs were respectively plated into a 96-well-plate and the immunized mouse serum, which includes anti-ESAT-6 and complement, was added to the wells at concentration of 1:10 dilution. Cells were incubated for 1 hour and washed two times with PBS, and then 20 mg/ml 7-amino actinomycin D (7-AAD) was added to each well for 20 min at 4°C in the dark. CDC activity was analyzed by Flow Cytometry (FCM, BD Company, USA) [16, 28, 29].

Assays of cytotoxicities of NK cells and splenocytes

At the end of the experiments, the spleen tissues were harvested from the mice immunized with the different vaccines. 5×10^6 splenocytes were labeled with 0.5 mM 5-(and 6)-carboxy-fluorescein diacetate succinimidyl ester (CFSE; 20 µg/ml) at 37°C for 15 min. The splenocytes were washed twice in PBS containing 5% fetal bovine serum to sequester any free CFSE. The CFSE-labeled splenocytes as effector cells were seeded with a constant number of YAC-1 target cells (for detecting NK cell cytotoxicity) or B16F10 target cells (for detecting splenocyte cytotoxicity) in a 96-well plate at 30:1 ratios of effector cells to target cells. The cytotoxicity activities were analyzed by FCM (BD company,

USA). All cytotoxicity assays were performed in triplicate, and was repeated twice [16, 30].

Histologic analysis

The lung tissues were harvested from the immunized mice at the end of the experiments, and fixed with 10% formalin, paraffin embedded and stained with hematoxylin and eosin (H&E) staining to observe the histo-pathological alterations. The slides were observed under the light microscope with 100 or 400× magnifications. Arrows represent the metastatic melanoma cells [31].

Western blot

Approximately 1×10^6 cells or tumor tissues were collected and lysed in the protein extraction buffer (Novagen, Madison, WI, USA) by following the manufacturer's protocol. Protein (15 mg/lane) was separated by SDS/PAGE (12% gels) and transferred on to nitrocellulose membranes. The membranes were blocked with saturating buffer for 1 h at 25°C, then followed by specific antibodies: goat anti-mouse IL-21 (I-18, Santa Cruz Biotechnology Company), the rabbit anti-mouse/human Vimentin and E-cadherin (Bioworld Technology, USA), respectively for overnight at 4°C. The membrane was rinsed for 5 min with an antibody wash solution for 3 times before adding to it the rabbit anti-goat or the goat anti-rabbit fluorescence secondary antibody. Immunoreactive bands were detected by Odyssey scanning instrument (LI-COR Odyssey Imaging System, USA). Protein quantitation was calculated using Image Lab software developed by Bio-Rad [41].

Statistical analysis

Data are shown as the average of ±S.D. for at least three independent experiments. Differences between test and control conditions were assessed by Student's t test analysis. Bonferroni correction was used where multiple comparisons were made. Statistically significant difference is indicated by: * when $p < 0.05$, ** when $p < 0.01$ and *** when $p < 0.003$.

Results

Identification of ESAT-6-gpi/IL-21 expression and analysis of isolated CD133+CD44+ cells

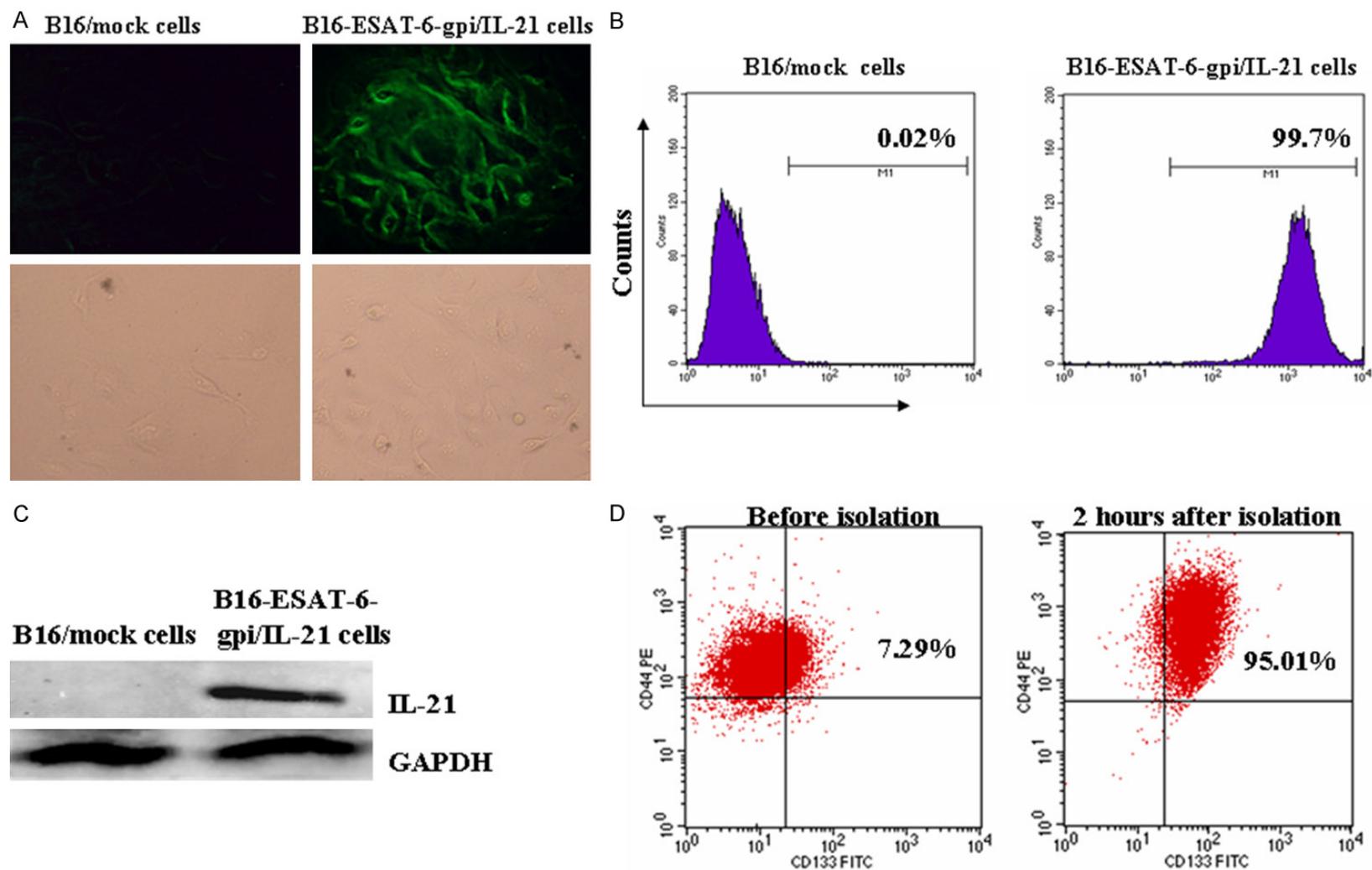To identify the expression of ESAT-6-gpi and IL-21 in previously engineered B16F10-ESAT-6-

Figure 1. B16F10-ESAT-6-gpi/IL-21 cells express target protein and CD133⁺CD44⁺ cells show a high purity. A. Image of green fluorescence represents the B16F10-ESAT-6-gpi/IL-21 cells in top right panel but not in B16F10/mock cells (top left one); in the bottom panels, cell images were seen under a light microscope. B. 99.7% of anti-ESAT-6 binding rate in B16F10-ESAT-6-gpi/IL-21 cells was detected by FCM, however, there is almost no anti-ESAT-6 binding on the surface of B16F10/mock cells. C. IL-21 band was found in the B16F10-ESAT-6-gpi/IL-21 cells, but not in the B16F10/mock cells. D. The left panel indicates CD133⁺CD44⁺ double positive cells in the B16F10-ESAT-6-gpi/IL-21 cells without isolation, and the right one indicates CD133⁺CD44⁺ double positive cells two hours after the cells were sorted by using MACS method.
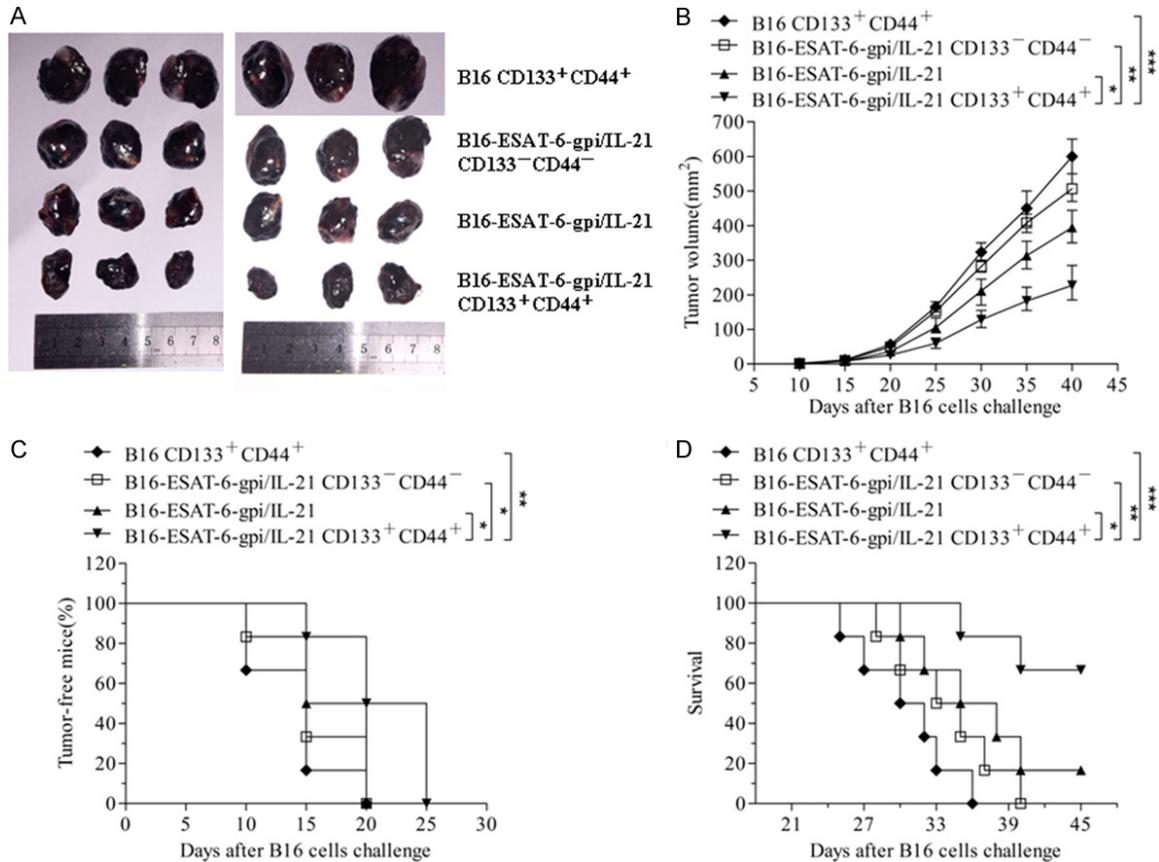
Figure 2. Inhibition of tumor-growth by B16F10-ESAT-6-gpi/IL-21 CD133⁺CD44⁺ CSC vaccine in mice. A. Images shows the tumor sizes stripped from the differently vaccine immunized mice 40 days after mice were challenged with B16F10 cells. B. The quantification analysis of tumor volumes. C. Tumor free mice challenged with B16F10 cells for 25 days. D. Tumor bearing mouse survival. $*p < 0.05$, $**p < 0.01$ and $***p < 0.003$; refer to the statistically significant differences as indicated.

gpi/IL-21 cells, which were stably selected from RPMI containing 800 mg/ml G418, we used ESAT-6-monoclone antibody to incubate B16F10-ESAT-6-gpi/IL-21 cells and B16F10/mock cells for identifying the expression of ESAT-6-gpi by an immunofluorescence assay. The result showed that the B16F10-ESAT-6-gpi/IL-21 cells exhibited green fluorescence (**Figure 1A**, top right panel). This is because the rat anti-mouse ESAT-6 was labeled with fluorescein isothiocyanate that made the cells indicating green fluorescence under the fluorescence microscope. Further, FCM analysis showed an anti-ESAT-6 binding rate was accounting for 99.7% in B16F10-ESAT-6-gpi/IL-21 cells (**Figure 1B**, right panel). However, B16F10/mock cells did not exhibit green fluorescence (**Figure 1A**, top left panel), and few anti-ESAT-6 bound to B16F10/mock cells (**Figure 1B**, left one). Cell images of bottom panels in **Figure 1A** were observed under a light microscope. Furthermore, the IL-21 expression was determined by western blot analysis in B16F10-ESAT-6-gpi/IL-21 cells but not in B16F10/mock cells (**Figure 1B**). These results demonstrated that the ESAT-6 was exactly anchored on the cell surface via GPI, and IL-21 was indeed secreted in B16F10-ESAT-6-gpi/IL-21 cells.

Next, we isolated the CD133⁺CD44⁺ CSCs from B16F10-ESAT-6-gpi/IL-21 cells by using MACS method, and analyzed the cellular purity by FCM. **Figure 1D** indicates the CD133⁺CD44⁺ CSC double positive cells were accounting for 95.01% two hours after the cells were isolated, and CD133⁺CD44⁺ cells was remarkably elevated in contrast to the B16F10-ESAT-6-gpi/IL-21 cells (95.01% vs. 7.29%, $p < 0.001$). Thus, the MACS method is a feasible way for isolation of CD133⁺CD44⁺ cells from the B16F10-ESAT-6-gpi/IL-21 cells.
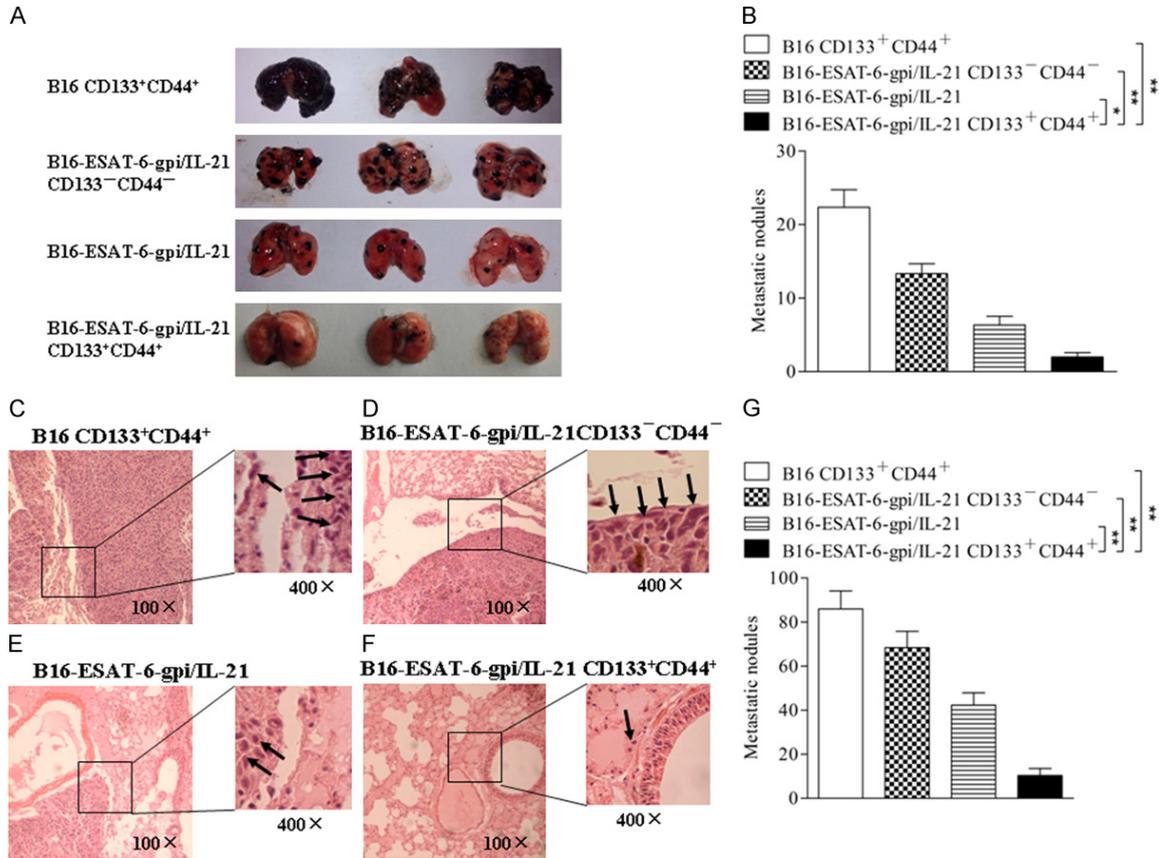
Figure 3. Evaluation of tumor lung metastasis by observation of tumor nodes and histological analysis. A. Images of tumor metastatic nodes in mouse lungs. B. The quantification analysis of lung tumor metastatic node counts. C-F. Tissue sections derived from the different vaccine immunized mice 40 days after challenged with the B16F10 cells, respectively. The arrows point to the metastatic focus (400×). G. Quantitative analysis of the tumor metastatic focus in lungs. *$p<0.05$, **$p<0.01$ and ***$p<0.003$; refer to the statistically significant differences as indicated.

Evaluation of B16F10-ESAT-6-gpi/IL-21 CD133+CD44+ CSC vaccine efficacy against melanoma in mice

Having identified the expression of ESAT-6-gpi and IL-21 in B16F10-ESAT-6-gpi/IL-21 cells as well as CD133+CD44+ cell purity, we used the B16F10-ESAT-6-gpi/IL-21 CD133+CD44+ cells as CSC-based vaccine inactivated with mitomycin C to evaluated this vaccine efficacy against melanoma in mice. Images of **Figure 2A** shows the tumor sizes on day 40 after the immunized mice were challenged with B16F10 cells. It was found that all mice immunized with the different tumor vaccines grew tumors in 25 days but the tumor volume, the time of tumor coming out, and the tumor bearing mouse survival days were obviously different among a various vaccine immunized mice. Although the effect of B16F10 CD133+CD44+ CSC vaccine on inhibition of tumor-growth was better than that of

B16F10 cell vaccine (data not shown), the CD133+CD44+ CSCs vaccinated mice fast generated tumors than that of mice vaccinated with other vaccines. Compared with other three group mice, the mice vaccinated with the B16F10-ESAT-6-gpi/IL-21 CD133+CD44+ CSC vaccine exhibited the best effect on melanoma, which was reflected in the smallest of tumor volume, the slowest of tumor coming out, and the longest of tumor bearing mouse survival as is shown in **Figure 2**.

In addition, the lung tissues were assessed by observation of tumor nodes. The B16F10-ESAT-6-gpi/IL-21 CD133+CD44+ CSC vaccine immunized mice inhibited the tumor cell pulmonary metastasis, and a few tumor nodes were found in the lung tissues 40 days after they were challenged with the B16F10 cells. The mice immunized with other vaccines generated more metastatic tumor nodes in the lung tissues than
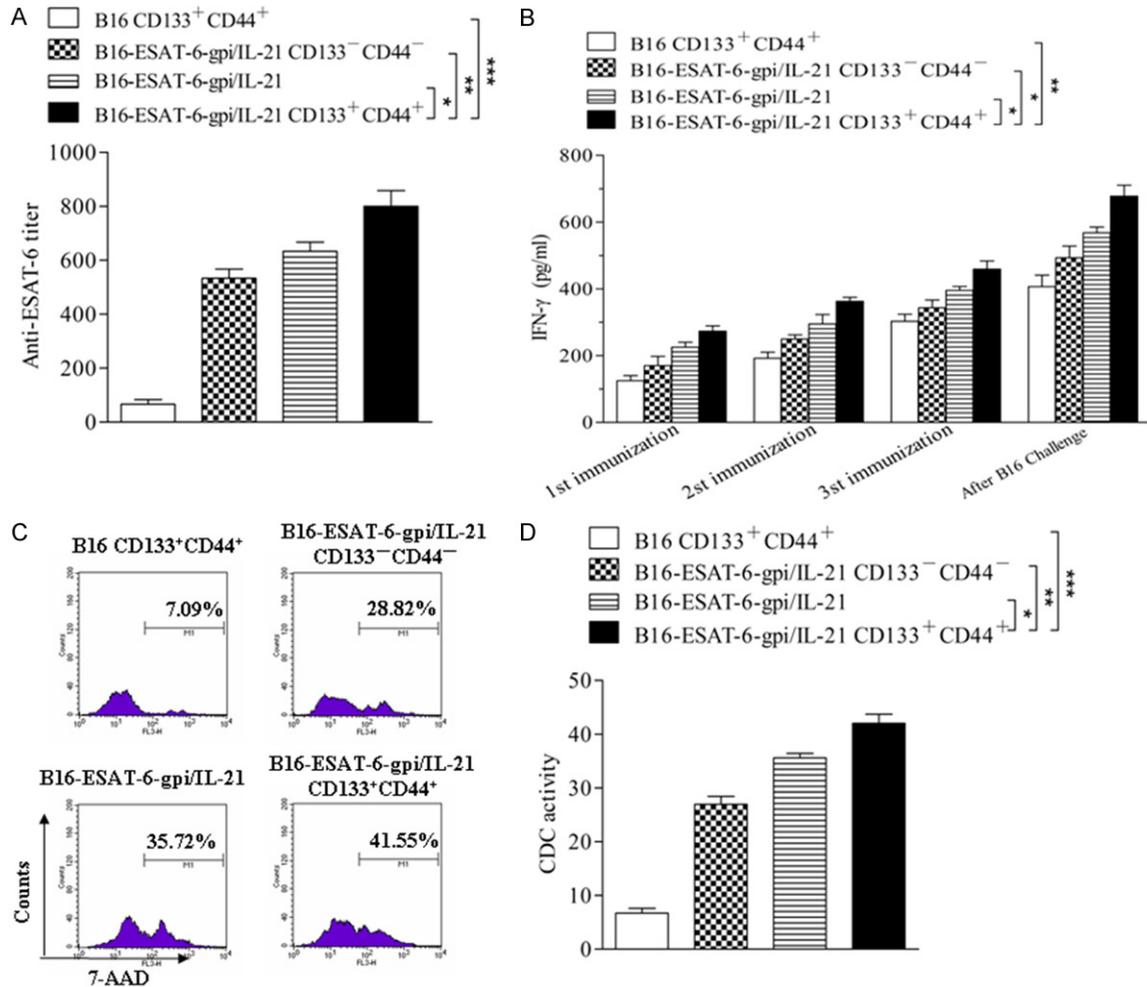
Figure 4. Serum levels of ESAT-6 antibody and IFN-g as well as CDC activity in the vaccinated mice. A, B. Serum levels of anti-ESAT-6 antibody and IFN-g were tested by enzyme linked immunosorbent assay. The mice were immunized s.c. with the various inactivated B16F10 vaccines and then were challenged by the B16F10 cells as described in the section of materials and methods. C. CDC activity was performed by using the various inactivated B16F10 vaccines and immunized mouse serum, and detected by FCM. D. Quantitative analysis of the CDC activity among 4 group vaccines. *$p<0.05$, **$p<0.01$ and ***$p<0.003$; refer to the statistically significant differences as indicated. Data are represented as mean +/- SEM (n=6).

that of B16F10-ESAT-6-gpi/IL-21 CD133⁺CD44⁺ CSC vaccine immunized mice as is shown in **Figure 3A**. The differences were statistically significant (**Figure 3B**). Consistently, the section of lung tissues in **Figure 3F** indicated a few metastatic focus seen (arrows) in the lungs from the mice immunized with B16F10-ESAT-6-gpi/IL-21 CD133⁺CD44⁺ CSC vaccine compared with the mice immunized with other vaccines (**Figure 3C-3E**). There were significant differences between the different vaccine groups (**Figure 3G**). It is thus evident from the results that the melanoma growth and metastasis were significantly inhibited in the mice vaccinated with B16F10-ESAT-6-gpi/IL-21 CD133⁺ CD44⁺ CSC vaccine.

B16F10-ESAT-6-gpi/IL-21 CD133⁺CD44⁺ CSC vaccine induces a strong immune responses in vaccinated mice challenged with B16F10 cells

To evaluate the immune efficacy of the different vaccines, we first measured the serum levels of anti-ESAT-6 antibody and IFN-γ. **Figure 4A** shows the anti-ESAT-6 titer was significantly increased in the B16F10-ESAT-6-gpi/IL-21 CD133⁺CD44⁺ CSC group compared with the B16F10-ESAT-6-gpi/IL-21 group (*$p<0.05$) or B16F10-ESAT-6-gpi/IL-21 CD133⁻CD44⁻ non CSC group (**$p<0.01$) or B16F10 CD133⁺ CD44⁺ CSC group (***$p<0.003$), and the serum anti-ESAT-6 antibody level in mice vacci-
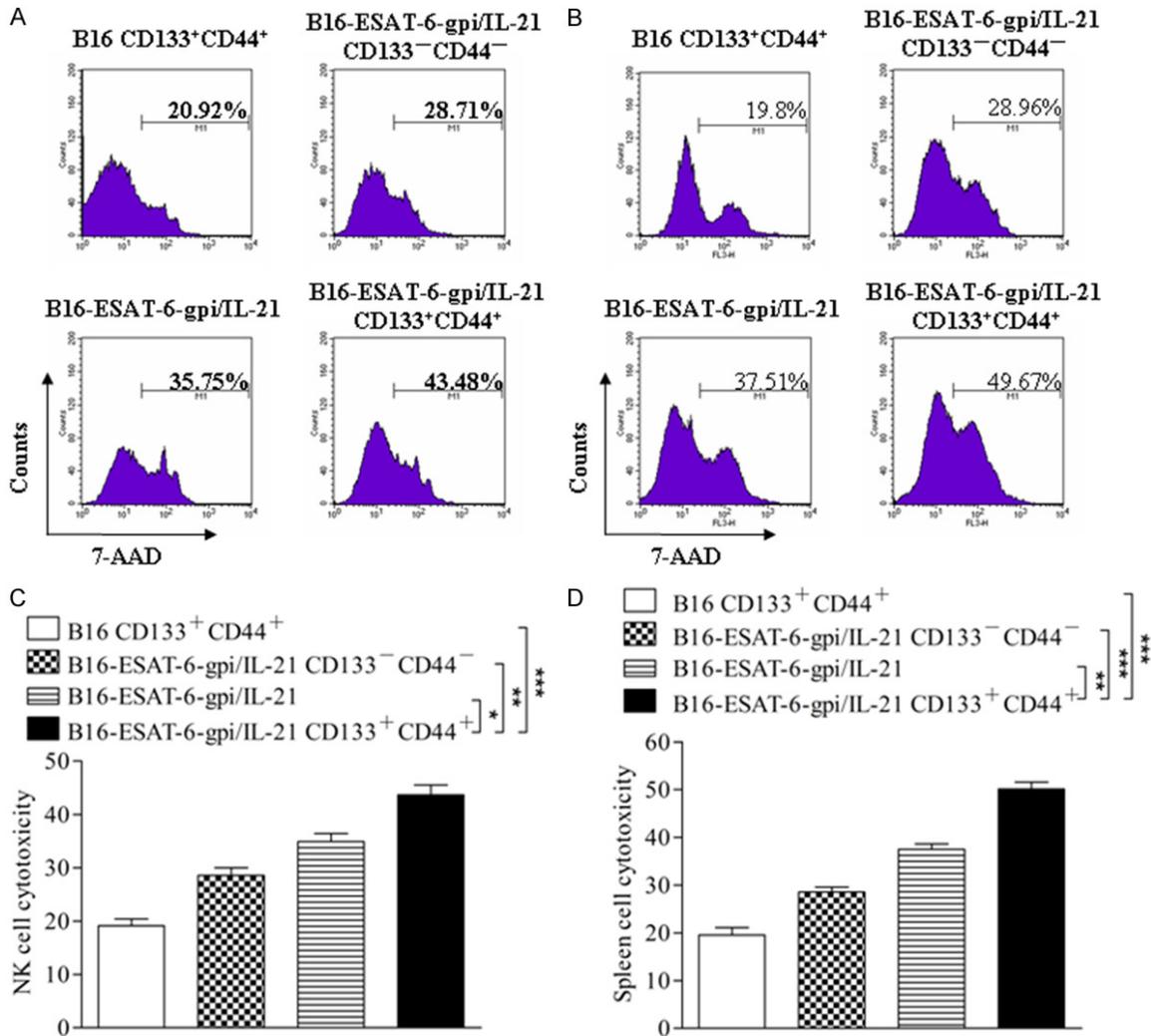
Figure 5. Cytotoxicities of NK cells and splenocytes analyzed by FCM. (A, B) FCM analysis results indicate the cytotoxicities of NK cells (A) and splenocytes (B) in mice immunized with the different vaccines, respectively. The ratio of the effector cells (splenocytes in the immunized mice) to the target cells (YAC-1 cells, NK cell cytotoxicity) or (B16F10 cells, splenocyte cytotoxicity) was 30:1. (C, D) A representative set of data for six mice were used to detect NK cytotoxicity and splenocyte cytotoxicity, respectively. An experiment was repeated twice. Statistically significant differences are indicated by asterisk for *$p<0.05$, **$p<0.01$, and ***$p<0.003$.

nated with the B16F10-ESAT-6-gpi/IL-21 was also significantly increased compared to the B16F10 CD133+CD44+ CSC group (**$p<0.01$). **Figure 4B** shows the serum IFN-g levels were dynamically increased. It was found that the IFN-γ level was gradually increased every immunization as well as after B16F10 cell challenge, especially in B16F10-ESAT-6-gpi/IL-21 CD133+ CD44+ CSC group. The differences were statistically significant in B16F10-ESAT-6-gpi/IL-21 CD133+CD44+ CSC group in contrast with the B16F10-ESAT-6-gpi/IL-21 group (*$p<0.05$), B16F10-ESAT-6-gpi/IL-21 CD133-CD44- non

CSC group (*$p<0.01$), and B16F10 CD133+ CD44+ CSC group (**$p<0.01$), respectively. Additionally, the CDC activity was markedly enhanced in the B16F10-ESAT-6-gpi/IL-21 CD133+CD44+ CSC group (***$p<0.003$) or in the B16F10-ESAT-6-gpi/IL-21 CD133-CD44- non CSC group (**$p<0.01$) or B16F10-ESAT-6-gpi/IL-21 group (*$p<0.05$) in contrast to the B16F10 CD133+CD44+ CSC group (**Figure 4C**, **4D**). These results indicate that the CSC vaccine B16F10-ESAT-6-gpi/IL-21 CD133+CD44+ cells could elicit a specific antibody response to ESAT-6, and a high level cytokine for serum
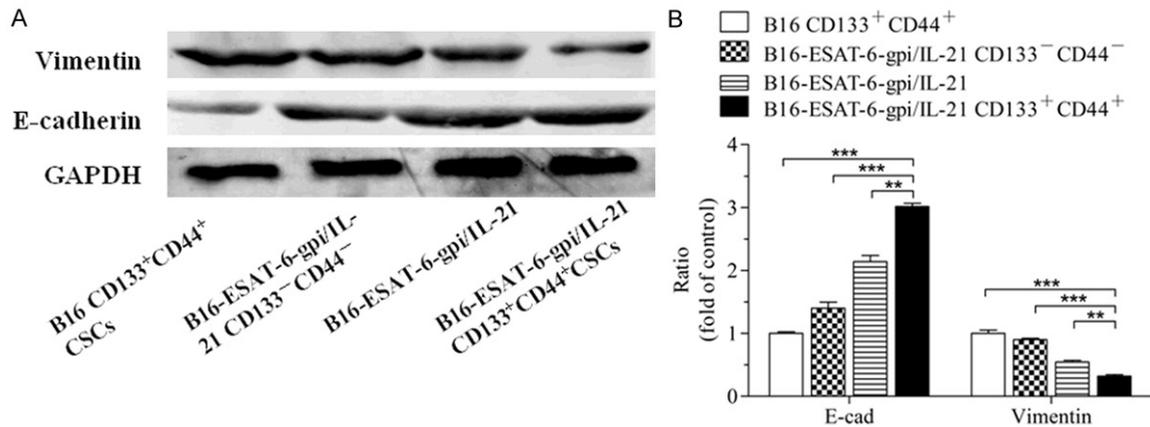
Figure 6. EMT-related molecular expression in the tumor tissues from the different vaccine immunized mice challenged with B16F10 cells. A. Expression of N-cadherin and E-cadherin in the tumor tissues analyzed by Western blot assay. B. Semi-quantification analysis of molecular expression; $**p<0.01$ and $***p<0.003$; refer to the statistical differences as indicated.

IFN-γ as well as a high activity of complement dependent cytotoxicity (CDC) in the vaccinated mice.

Analysis of cytotoxicities of NK cells and splenocytes in the vaccinated mice challenged with B16F10 cells

Since the cytotoxicity of immune cells may serve as a key power to fight tumor cells, we therefore analyzed the cytotoxicities of NK cells and splenocytes in the vaccinated mice in four separate experiments. In **Figure 5A**, the NK cell cytotoxic activity (splenocytes against target cells YAC-1) in the B16F10-ESAT-6-gpi/IL-21 CD133+CD44+ CSC vaccine group was the highest (43.48%) among 4 group vaccines, and the B16F10-ESAT-6-gpi/IL-21 group ranked second (35.75%). The lowest NK cytotoxic activity was in the B16F10 CD133+CD44+ CSC group (20.92%). There were significant differences between the first 2 high cytotoxicity groups (*$p<0.05$), between the B16F10-ESAT-6-gpi/IL-21 CD133+CD44+ CSC and the B16F10 CD133+CD44+ CSC groups (***$p<0.003$), and between the B16F10-ESAT-6-gpi/IL-21 CD133+CD44+ CSC and the B16F10-ESAT-6-gpi/IL-21 CD133-CD44- non CSC groups (**$p<0.01$) as is shown in **Figure 5C**. The splenocyte cytotoxic activity (splenocytes against target cells B16F10) shown in **Figure 5B** was also true. The statistical significance is shown in **Figure 5D**. From these results, we concluded that the CSC vaccine B16F10-ESAT-6-gpi/IL-21 CD133+CD44+ cells could induce strong cell mediated immunity against melanoma.

Expression of N-cadherin and E-cadherin in the tumor tissue from the vaccinated mice challenged with B16F10 cells

To analyze the mechanisms of the B16F10-ESAT-6-gpi/IL-21 CD133+CD44+ CSC vaccine for inhibiting tumor cell metastases, we detected the expression of E-cadherin and Vimentin, a characteristic molecules of EMT that are closely associated with typical phenotype changes of EMT in tumor cell growth and metastasis [32]. **Figure 6A** shows the results of the western blot, the samples from the tumor tissues in the mice that received different vaccines. Compared with those from other vaccine groups, the Vimentin expression was significantly decreased whereas E-cadherin expression was significantly increased in the tumor tissues from the mice vaccinated with B16F10-ESAT-6-gpi/IL-21 CD133+CD44+ CSC vaccine. There were significant differences between the different vaccine groups as is shown in **Figure 6B**.

Discussion

A major obstacle to the success of any form of specific tumor vaccine might be the tumors that escape from immune recognition. Mycobacterium tuberculosis antigen ESAT-6 is an xenogeneic antigen that is a little bit of similarity to mutated melanoma antigens [11, 33-35]. ESAT-6 anchored by the GPI and exposure to surface of tumor cells, in our developed the B16F10-ESAT-6-gpi/IL-21 CD133+CD44+ CSC vaccine, may provide a form of antigen that the

immune system perceives as foreign, which in turn elicits melanoma-specific immune responses in a mouse model. IL-21 is a T cell-derived cytokine that regulates the immune responses in developing tumor vaccine as adjuvant molecule [36]. Importantly, CSCs may be more effective immunogenic as an antigen source than unselected non CSCs in inducing antitumor immune responses. Thus, CSC-based vaccination confers significant antitumor immunity, whereas no targeting CSCs may be a significant factor contributing to treatment failure [21, 22, 37]. To this end, we assessed the anti-melanoma efficacy of B16F10-ESAT-6-gpi/IL-21 CD133+CD44+ CSC vaccine on melanoma bearing mice in this study.

Comparative analysis of different vaccine efficacy against melanoma indicates that the B16F10-ESAT-6-gpi/IL-21 CD133+CD44+ CSC vaccine did induce a powerful antitumor immune responses to inhibit melanoma growth and lung metastasis after challenged with the B16F10 cells in the mouse melanoma syngeneic model, which was reflected in efficiently reducing tumor volume, postponing occurrence time, and extending survival of tumor bearing mice as well as decreasing pulmonary tumor nodes. We also observed the anti-melanoma efficacy of CD133+CD44+ CSC-based vaccine without expressing ESAT-6-gpi and secreting IL-21 was the lowest among all tested vaccines in spite of better than B16F10 cell vaccine (data not shown), suggesting CSC-based vaccine alone was not enough to elicit a strong antitumor immune responses against melanoma in mouse model. The possible mechanism is that B16F10-ESAT-6-gpi/IL-21 CD133-CD44- non CSC and B16F10-ESAT-6-gpi/IL-21 vaccines expressed the ESAT-6 to stimulate the generation of antibody that binds to CSCs. This will result in CSC lysis in the presence of complement, whereas CSC-based vaccine alone lacks ESAT-6 and the molecular adjuvant IL-21, which promote the IFN-γ secreting and enhance the cytotoxicity activity, leading to strong antitumor immunity in the tumor vaccine. This may explained the non-efficient inhibition of melanoma growth and metastasis in mice immunized with CSC-based vaccine alone.

An immunogenic cancer cell death (ICD) is originally observed during the treatment with several chemotherapeutics or ionizing irradiation, and has revolutionized the view on the antican-

cer therapies [38]. Based on concept of ICD, we guess that the serum anti-ESAT-6 antibody in the immunized mice might have bound the Fc γ receptor of NK cells to activate NK cells, which resulted in antibody dependent cell cytotoxicity (ADCC). The CSC vaccine B16F10-ESAT-6-gpi/IL-21 CD133+CD44+ cells, therefore, may be killed by CDC, ADCC and splenocyte cytotoxicity. ICD cells served as a potential potent trigger for tolerance break to elicit an initiation of naturally antimelanoma immunity through reactive oxygen species generation, endoplasmic reticulum stress response, and emission of danger-associated molecular patterns [39-41]. In addition, ICD cells might be an excellent source for dendric cell loading when ICD cells bound specific serum antibody to form ICD cell immune complex. This complex may serve as potential uncharacterized antigens that efficiently presented to T lymphocytes for eliciting lymphocyte cytotoxicity against melanoma cells [10, 40].

To understand the mechanisms of the inhibiting melanoma metastasis, we analyzed the EMT-associated molecule expression. EMT is a process that exerts influence on many molecules in cancer process. The E-cadherin and Vimentin respectively represent the characteristic molecules of cellular epithelium and mesenchyma state conversion [23, 41, 42]. The findings from Western blot analysis showed that the Vimentin was markedly decreased, whereas the E-cadherin was obviously increased in tumor tissues from the mice immunized with the B16F10-ESAT-6-gpi/IL-21 CD133+CD44+ CSC vaccine compared with other vaccine immunized mice. This result may elucidate why the metastatic tumor nodes in lungs were less found in mice immunized with the B16F10-ESAT-6-gpi/IL-21 CD133+CD44+ CSC vaccine. Surprisingly, the analysis result of the histo-pathological alterations from the section of lung tissues was consistent with the observation result of metastatic tumor nodes from lung tissues. While it remains unknown why vaccination of the B16F10-ESAT-6-gpi/IL-21 CD133+CD44+ CSC is better than that of the B16F10-ESAT-6-gpi/IL-21, further investigations are needed to obtain better insights into the mechanisms of the CSC-based vaccines in cancer progression and metastasis.

In conclusion, this preliminary study represents the first attempt to demonstrate that CSC-

based vaccine induces immune responses and results in a significant inhibition of melanoma growth and metastases. Although the cellular and molecular mechanisms underlying this anti-melanoma effects are still poorly understood, CSC-based vaccine modified by xenogeneic antigen and molecular adjuvant clearly demonstrates an attractive therapeutic approach to restore immune competence in melanoma bearing individuals.

Disclosure of conflict of interest

None.

Address correspondence to: Dr. Jun Dou, Department of Pathogenic Biology and Immunology, School of Medicine, Southeast University, Dingjiaqiao 87#, Nanjing 210009, China. E-mail: njdoujun@seu.edu.cn

References

[1] Patel KR, Lawson DH, Kudchadkar RR, Carthon BC, Oliver DE, Okwan-Duodu D, Ahmed R, Khan MK. Two heads better than one? Ipilimumab immunotherapy and radiation therapy formelanoma brain metastases. Neuro Oncol 2015; 17: 1312-1321.

[2] Kotobuki Y, Yang L, Serada S, Tanemura A, Yang F, Nomura S, Kudo A, Izuhara K, Murota H, Fujimoto M, Katayama I, Naka T. Periostin accelerates human malignant melanoma progression by modifying the melanoma microenvironment. Pigment Cell Melanoma Res 2014; 27: 630-639.

[3] Romano S, Staibano S, Greco A, Brunetti A, Nappo G, Ilardi G, Martinelli R, Sorrentino A, Di Pace A, Mascolo M, Bisogni R, Scalvenzi M, Alfano B, Romano MF. FK506 binding protein 51 positively regulates melanoma stemness and metastatic potential. Cell Death Dis 2013; 4: e578.

[4] Schadendorf D, Paschen A, Sun Y. Autologous, allogeneic tumor cells or genetically engineered cells as cancer vaccine against melanoma. Immunol Lett 2000; 74: 67-74.

[5] Clancy-Thompson E, Perekslis TJ, Croteau W, Alexander MP, Chabanet TB, Turk MJ, Huang YH, Mullins DW. Melanoma Induces, and Adenosine Suppresses, CXCR3-Cognate Chemokine Production and T-cell Infiltration of Lungs Bearing Metastatic-like Disease. Cancer Immunol Res 2015; 3: 956-967.

[6] Esfandiary A, Ghafouri-Fard S. MAGE-A3: an immunogenic target used in clinical practice. Immunotherapy 2015; 7: 683-704.

[7] Atkins MB. Cytokine-based therapy and biochemotherapy for advanced melanoma. Clin Cancer Res 2006; 12: 2353s-8s.

[8] Polak ME, Borthwick NJ, Jager MJ, Cree IA. Melanoma vaccines: the problems of local immunosuppression. Hum Immunol 2009; 70: 331-339.

[9] He X, Wang J, Zhao F, Chen D, Chen J, Zhang H, Yang C, Liu Y, Dou J. ESAT-6-gpi DNA vaccine augment the specific anti-tumor efficacy induced by the tumor vaccine B16F10-ESAT-6-gpi/IL-21 in mice model. Scand J Immunol 2013; 78: 69-78.

[10] Restifo NP. Building better vaccines: how apoptotic cell death can induce inflammation and activate innate and adaptive immunity. Curr Opin Immunol 2000; 12: 597-603.

[11] Carreno BM, Magrini V, Becker-Hapak M, Kaabinejadian S, Hundal J, Petti AA, Ly A, Lie WR, Hildebrand WH, Mardis ER, Linette GP. Cancer immunotherapy dendritic cell vaccine increases the breadth and diversity of melanoma neoantigen-specific T cells. Science 2015; 348: 803-808.

[12] Ganguly N, Giang PH, Basu SK. Mycobacterium tuberculosis 6-kDa early secreted antigenic target (ESAT-6) protein downregulates lipopolysaccharide induced c-myc expression by modulating the extracellular signal regulated kinases 1/2. BMC Immunol 2007; 8: 24.

[13] Dou J, Wang Y, Yu F, Yang H, Wang J, He X, Xu W, Chen J, Hu K. Protection against Mycobacterium tuberculosis challenge in mice by DNA vaccine Ag85A-ESAT-6-IL-21 priming and BCG boosting. Int J Immunogenet 2012; 39: 183-190.

[14] Croce M, Rigo V, Ferrini S. IL-21: a pleiotropic cytokine with potential applications in oncology. J Immunol Res 2015; 2015: 696578.

[15] Ji JF, Li J H, Lillia MH. Synergistic anti-tumor effect of glycosylphosphatidylinositol- anchored IL-2 and IL-12. J Gene Med 2004; 6: 777-785.

[16] Zhao F, Dou J, He XF, Wang J, Chu L, Hu W, Yu F, Hu K, Wu Y, Gu N. Enhancing therapy of B16F10 melanoma efficacy through tumor vaccine expressing GPI-anchored IL-21 and secreting GM-CSF in mouse model. Vaccine 2010; 28: 2846-2852.

[17] Vaibhav S, Robert H S. Potential for therapeutic targeting of tumor stem cells. Cancer Sci 2010; 101: 16-21.

[18] Wang J, Cao MG, You CZ, Wang CL, Liu SL, Kai C, Dou J. A preliminary investigation of the relationship between circulating tumor cells and cancer stem cells in patients with breast cancer. Cell Mol Biol (Noisy-le-grand) 2012; 58 Suppl: OL1641-1645.

[19] Yu Y, Ramena G, Elble RC. The role of cancer stem cells in relapse of solid tumors. Front Biosci (Elite Ed) 2012; 4: 1528-1541.

[20] Pan Q, Li Q, Liu S, Ning N, Zhang X, Xu Y, Chang AE, Wicha MS. Concise Reviews: Targeting Cancer Stem Cells Using Immunologic Approaches. Stem Cells 2015; 33: 2085-2892.

[21] Ning N, Pan Q, Zheng F, Teitz-Tennenbaum S, Egenti M, Yet J, Li M, Ginestier C, Wicha MS, Moyer JS, Prince ME, Xu Y, Zhang XL, Huang S, Chang AE, Li Q. Cancer stem cell vaccination confers significant antitumor immunity. Cancer Res 2012; 72: 1853-1864.

[22] Duarte S, Momier D, Baqué P, Casanova V, Loubat A, Samson M, Guigonis JM, Staccini P, Saint-Paul MC, De Lima MP, Carle GF, Pierrefite-Carle V. Preventive cancer stem cell-based vaccination reduces liver metastasis development in a rat colon carcinoma syngeneic model. Stem Cells 2013; 31: 423-432.

[23] Lu L, Tao H, Chang AE, Hu Y, Shu G, Chen Q, Egenti M, Owen J, Moyer JS, Prince ME, Huang S, Wicha MS, Xia JC, Li Q. Cancer stem cell vaccine inhibits metastases of primary tumors and induces humoral immune responses against cancer stem cells. Oncoimmunology 2015; 4: e990767.

[24] Dou J, Pan M, Wen P, Li Y, Tang Q, Chu L, Zhao F, Jiang C, Hu W, Hu K, Gu N. Isolation and identification of cancer stem-like cells from murine melanoma cell lines. Cell Mol Immunol 2007; 4: 467-72.

[25] Yang C, Xiong F, Wang J, Dou J, Chen J, Chen D, Zhang Y, Luo S, Gu N. Anti-ABCG2 Monoclonal Antibody in Combination with Paclitaxel-Nanoparticles Against Cancer Stem-like Cell Activity in Multiple Myeloma. Nanomedicine (Lond) 2014; 9: 45-60.

[26] Chen D, Zhang Y, Wang J, Chen J, Yang C, Cai K, Wang X, Shi F, Dou J. MicroRNA-200c overexpression inhibits tumorigenicity and metastasis of CD117+CD44+ ovarian cancer stem cells by regulating epithelial- mesenchymal transition. J Ovarian Res 2013; 6: 50.

[27] Rosenberg SA, Sherry RM, Morton KE. Tumor progression can occur despite the induction of very high levels of self/tumor antigen-specific CD8+T cells in patients with melanoma. J Immunol. 2005; 175: 6169-76.

[28] Atanackovic D, Panse J, Hildebrandt Y. Surface molecule CD229 as a novel target for the diagnosis and treatment of multiple myeloma. Haematologica 2011; 96: 1512-1520.

[29] Hervé L, Michèle F, Sylvie G. A novel flow cytometric assay for quantitation and multiparametric characterization of cell-mediated cytotoxicity. J Immunol Methods 2001; 253: 177-187.

[30] Wang X, Zhao F, He X, Wang J, Zhang Y, Zhang H, Ni Y, Sun J, Wang X, Dou J. Combining TGF-β1 knockdown and miR200c administration to optimize antitumor efficacy of B16F10/GPI-IL-21 vaccine. Oncotarget 2015; 6: 12493-12504.

[31] Hu W, Wang J, Dou J, He X, Zhao F, Jiang C, Yu F, Hu K, Chu L, Li X, Gu N. Augmenting Therapy of Ovarian Cancer Efficacy by Secreting IL-21Human Umbilical Cord Blood Stem Cells in Nude Mice. Cell Transplant 2011; 20: 669-680.

[32] Burk U, Schubert J, Wellner U, Schmalhofer O, Vincan E, Spaderna S, Brabletz T. A reciprocal repression between ZEB1 and members of the miR-200 family promotes EMT and invasion in cancer cells. EMBO Rep 2008; 9: 582-589.

[33] Wölfel T, Hauer M, Schneider J, Serrano M, Wölfel C, Klehmann-Hieb E, De Plaen E, Hankeln T, Meyer zum Büschenfelde KH, Beach D. p16INK4a-insensitive CDK4 mutant targeted by cytolytic T lymphocytes in a human melanoma. Science 1995; 269: 1281-1284.

[34] Robbins PF, Lu YC, El-Gamil M, Li YF, Gross C, Gartner J, Lin JC, Teer JK, Cliften P, Tycksen E, Samuels Y, Rosenberg SA. Mining exomic sequencing data to identify mutated antigens recognized by adoptively transferred tumor-reactive T cells. Nat Med 2013; 19: 747-752.

[35] Fedosova NI, Voeykova IM, Karaman OM, Symchych TV, Didenko GV, Lisovenko GS, Evstratieva LM, Potebnia GP. Cytotoxic activity of immune cells following administration of xenogeneic cancer vaccine in mice with melanoma B-16. Exp Oncol 2015; 37: 130-134.

[36] Smyth MJ, Teng MW, Sharkey J. Interleukin 21 enhances antibody-mediated tumor rejection. Cancer Res 2008; 68: 3019-3025.

[37] Teitz-Tennenbaum S, Wicha MS, Chang AE, Li Q. Targeting cancer stem cells via dendritic-cell vaccination. Oncoimmunology 2012; 1: 1401-1403.

[38] Adkins I, Fucikova J, Garg AD, Agostinis P, Špíšek R. Physical modalities inducing immunogenic tumor cell death for cancer immunotherapy. Oncoimmunology 2015; 3: e968434.

[39] Akiyama K, Shin E, Ayumi Y. Targeting Apoptotic Tumor Cells to FcgR Provides Efficient and Versatile Vaccination Against Tumors by Dendritic Cells. J Immunol 2003; 170: 1641-1648.

[40] He X, Wang J, Zhao F, Yu F, Chen D, Cai K, Yang C, Chen J, Dou J. Anti-tumor Efficacy of Viable Tumor Vaccine Modified by Heterogenetic ESAT-6 Antigen and Cytokine IL-21 in

Melanomatous Mouse. Immunol Res 2012; 52: 240-249.

[41] Alexaki VI, Javelaud D, Van Kempen LC, Mohammad KS, Dennler S, Luciani F, Hoek KS, Juàrez P, Goydos JS, Fournier PJ, Sibon C, Bertolotto C, Verrecchia F, Saule S, Delmas V, Ballotti R, Larue L, Saiag P, Guise TA, Mauviel A. GLI2-Mediated Melanoma Invasion and Metastasis. J Natl Cancer Inst 2010; 102: 1148-1159.

[42] Liu S, Tetzlaff MT, Liu A, Liegl-Atzwanger B, Guo J, Xu X. Loss of microRNA-205 expression is associated with melanoma progression. Lab Invest 2012; 92: 1084-1096.